THE JOURNAL OF BIOLOGICAL CHEMISTRY VOL. 290, NO. 14, pp. 8711–8721, April 3, 2015

Fatty Acid-binding Proteins (FABPs) Are Intracellular Carriers for Δ^9-Tetrahydrocannabinol (THC) and Cannabidiol (CBD)*

Received for publication, October 15, 2014, and in revised form, February 2, 2015 Published, JBC Papers in Press, February 9, 2015, DOI 10.1074/jbc.M114.618447

Matthew W. Elmes[‡1], Martin Kaczocha[‡§1], William T. Berger[¶1], KwanNok Leung[‡], Brian P. Ralph[‡], Liqun Wang[‡], Joseph M. Sweeney[‡], Jeremy T. Miyauchi[‖], Stella E. Tsirka[‖], Iwao Ojima[¶], and Dale G. Deutsch[‡2]

From the Departments of [‡]Biochemistry and Cell Biology, [§]Anesthesiology, and [¶]Chemistry, the Institute of Chemical Biology and Drug Discovery, and the [‖]Department of Pharmacological Sciences, Stony Brook University, Stony Brook, New York 11795-5215

Background: Δ^9-Tetrahydrocannabinol (THC) and cannabidiol (CBD) modulate endocannabinoid tone *in vivo* through unknown mechanisms.
Results: THC and CBD bind to fatty acid-binding proteins (FABPs) and reduce endocannabinoid metabolism. Neither THC nor CBD inhibit human fatty acid amide hydrolase activity.
Conclusion: FABPs are intracellular transporters of THC and CBD.
Significance: These findings identify a new mechanism by which phytocannabinoids influence endocannabinoid signaling.

Δ^9-Tetrahydrocannabinol (THC) and cannabidiol (CBD) occur naturally in marijuana (*Cannabis*) and may be formulated, individually or in combination in pharmaceuticals such as Marinol or Sativex. Although it is known that these hydrophobic compounds can be transported in blood by albumin or lipoproteins, the intracellular carrier has not been identified. Recent reports suggest that CBD and THC elevate the levels of the endocannabinoid anandamide (AEA) when administered to humans, suggesting that phytocannabinoids target cellular proteins involved in endocannabinoid clearance. Fatty acid-binding proteins (FABPs) are intracellular proteins that mediate AEA transport to its catabolic enzyme fatty acid amide hydrolase (FAAH). By computational analysis and ligand displacement assays, we show that at least three human FABPs bind THC and CBD and demonstrate that THC and CBD inhibit the cellular uptake and catabolism of AEA by targeting FABPs. Furthermore, we show that in contrast to rodent FAAH, CBD does not inhibit the enzymatic actions of human FAAH, and thus FAAH inhibition cannot account for the observed increase in circulating AEA in humans following CBD consumption. Using computational molecular docking and site-directed mutagenesis we identify key residues within the active site of FAAH that confer the species-specific sensitivity to inhibition by CBD. Competition for FABPs may in part or wholly explain the increased circulating levels of endocannabinoids reported after consumption of cannabinoids. These data shed light on the mechanism of action of CBD in modulating the endocannabinoid tone *in vivo* and may explain, in part, its reported efficacy toward epilepsy and other neurological disorders.

Cannabis sativa contains more than 100 known cannabinoids, including Δ^9-tetrahydrocannabinol (THC)[3] and cannabidiol (CBD). THC and CBD are mainly formed from marijuana when their corresponding acids are decarboxylated upon heating (1). THC is thought to act primarily via the activation of specific cannabinoid receptors, CB_1 and CB_2 (2). Unlike THC, CBD does not serve as a CB receptor agonist and binds to CB receptors with very low affinity (3). CBD is non-psychoactive, however, its pharmacological use has been shown to exert anti-inflammatory, anti-convulsant, anxiolytic, and neuroprotective effects in a CB receptor-independent manner (2, 4, 5). The mechanism of action of CBD is still a matter of some debate, however, there is evidence that its anxiolytic, neuroprotective, and antidepressant effects are mediated by its ability to activate 5-HT_{1A} receptors (6–8).

THC and CBD are hydrophobic and are transported in the blood by lipoproteins and albumin (9, 10). However, intracellular transporters for phytocannabinoids have not been described. In theory these hydrophobic compounds may be transported from the cell membrane through the aqueous milieu by soluble intracellular carriers. The fatty acid-binding proteins (FABPs) have been shown to be intracellular transporters for the endocannabinoid anandamide (AEA) and other *N*-acylethanolamines (11–13). AEA requires transport from the membrane to intracellular fatty acid amide hydrolase (FAAH) for inactivation (11, 14, 15). Inhibitors of the FABPs have recently been shown to raise brain levels of AEA by limiting its transport into the cell to FAAH (11, 12, 16). Similar observations of heightened blood and brain anandamide concentrations following consumption of phytocannabinoids have been made, however, the mechanism of action is unclear (17). The mammalian brain expresses three FABP subtypes: FABP3, FABP5, and FABP7 (18). Here, we examine whether cannabinoids also bind to the FABPs and, as such, act as inhibitors of anandamide inactivation.

* This work was supported, in whole or in part, by National Institutes of Health Grants DA032232, DA035923, DA035949, DA016419, DA026593, GM007518, GM008444, and NS042168.
[1] These authors contributed equally to this work.
[2] To whom correspondence should be addressed. Tel.: 631-632-8595; Fax: 631-632-8575; E-mail: Dale.Deutsch@Stonybrook.edu.

[3] The abbreviations used are: THC, Δ^9-tetrahydrocannabinol; CBD, cannabidiol; FABP, fatty acid-binding protein; 2-AG, 2-arachidonoylglycerol; AEA, arachidonoylethanolamide; FAAH, fatty acid amide hydrolase; PDB, Protein Data Bank; MD, molecular dynamics.

EXPERIMENTAL PROCEDURES

Chemicals

AEA was from Cayman Chemical (Ann Arbor, MI), THC, CBD, and fatty acid-free BSA were from Sigma, [^{14}C]AEA (arachidonoyl-[1-^{14}C]ethanolamide, 60 mCi/mmol) was provided by the Drug Supply Program at the National Institute on Drug Abuse.

Cell Culture and Transfections

Wild-type and FABP5 shRNA-expressing HeLa cells (12) were grown in DMEM supplemented with 10% fetal bovine serum, 100 units/ml of penicillin/streptomycin, 2 mM L-glutamine, and 1 mM sodium pyruvate. Transfections of human FAAH were carried out using the GenJet Plus reagent (SignaGen, Rockville, MD) according to the manufacturer's instructions.

In Vitro Binding of Ligands to FABPs

Binding analysis of THC and CBD to FABPs was carried out as described (14).

In Silico Studies

Initial Docking—THC and CBD were docked using DOCK version 6.5 (19). Energy grids were first generated using the grid program for the three FABP serotypes: FABP3 (Protein Data Bank (PDB) code 3RSW, 2.6-Å resolution), FABP5 (PDB code 1B56, 2.05-Å resolution), and FABP7 (PDB code 1FE3, 2.8-Å resolution) (20, 21). Likewise, energy grids were generated for the FAAH variants: rat FAAH (PDB code 3QJ8, 2.9-Å resolution), humanized FAAH (PDB code 2WAP, 2.8-Å resolution), and mutant FAAH (a variant created by introducing mutations F160L and M463V in 2WAP with UCSF Chimera v1.9) (22–24). Each ligand molecule was then flexibly docked to each of the respective FABP or FAAH grids (DOCK FLX protocol) (25) and the single lowest energy pose was retained. To generate comparative energy scores, the CBD pose generated in rat FAAH was fixed anchor docked to humanized FAAH and F160L/M463V mutant FAAH (DOCK FAD protocol) (25) and the single lowest energy pose was retained for each respective FAAH.

Simulation Setups and Molecular Dynamics—MD simulations were adapted from the methodology carried out in Ref.27. Each MD trajectory (2 ns) was performed using NAMD 2.9 (28) employing charmrun to assign multiple processors (~10) on the Seawulf Cluster at Stony Brook University. Preparation of each the initial MD coordinates started with docked complexes, which were subsequently stripped of crystallographic waters and prepared using the AMBER8 suite (*leap, antechamber*) (29). AMBER8 was used to assign force field parameters and solvate each complex in a periodic box containing ~5000 waters (~60 Å^3). Force fields were assigned independently using AMBER8: FF99SB (30) for the protein, GAFF for the ligand, and TIP3P (31) for the water. Prior to running each simulation, a nine-step equilibration of three minimization steps (2000 steps of steepest decent) and seven molecular dynamics runs (50 ps each) as described in Ref. 32 were performed to equilibrate the system before the production run (2 ns) (32).

MD simulations were carried out in the NPT ensemble using Langevin dynamics at a constant temperature of 310 K and constant pressure of 1.01325 bar (33). All MD simulations employed a 1-fs time step that required the use of SHAKE (34). Additional key parameters included particle mesh Ewald (35) to compute long-range electrostatics (1.5 Å grid spacing) and a 10-Å cutoff (8 Å smoothing switch) for non-bonded interactions. Each MD frame is composed of 1000 fp (1 ps) and was run for a total of 2 ns.

MMGBSA Calculations—Free energies of binding (ΔG_{bind} Calculated) were carried out using the MM-GBSA method (36, 37). All MM-GBSA calculation were carried out post production. For each complex, AMBER8 (*p-traj*) was employed to strip all explicit water from each of the 2-ns MD trajectories. A single point calculation was carried out using AMBER8 (*sander*) for each ps (2000 ps in 2 ns) with the following parameters: AMBER radii (*mbondi2*), Dielectric constants (1 and 78.5), and GB model (igb = 5) (38).

Following Equation 1, the MM-GBSA free energy of binding (ΔG_{bind}) was calculated using the non-bonded intermolecular protein-ligand interactions (ΔG_{coul} and ΔG_{vdw}), the change in hydration energy (ΔG_{hyd}), and the temperature multiplied by the change in solute vibrational, rotational, and translational entropy ($T\Delta S$).

$$\Delta G_{bind} = \Delta E_{coul} + \Delta E_{vdw} + \Delta\Delta G_{hyd} - T\Delta S \quad \text{(Eq. 1)}$$

Specifically, ΔG_{coul} and ΔG_{vdw} were calculated from the change in energy for all nonbonded intermolecular protein-ligand interactions (Coulombic and van deer Waals) as the receptor and ligand go from a free state to a bound state (complex) shown in Equation 2.

$$\Delta E_{coul/vdw} = \Delta E_{complex} - (\Delta E_{receptor} + \Delta E_{ligand}) \quad \text{(Eq. 2)}$$

The $\Delta\Delta G_{hyd}$ was calculated from the $\Delta G_{hyd} = G_{polar} + G_{nonpolar}$ for each species (complex, receptor, and ligand) as shown in Equation 3.

$$\Delta\Delta G_{hyd} = \Delta G_{hydcomplex} - (\Delta G_{hydreceptor} + \Delta G_{hydligand}) \quad \text{(Eq. 3)}$$

Furthermore, G_{polar} was calculated using the GB method and molecular solvent accessible surface (SASA) was used to calculate $G_{nonpolar} = \gamma \times \text{SASA} + \beta$ using standard constants (γ = 0.00542 kcal mol^{-1} Å^{-2} and β = 0.82 kcal/mol) (39). Entropy ($T\Delta S$) was calculated using quazi-harmonic normal mode analysis of energy minimized structures (see Entropy Calculation) at 310 K (37).

Calculation of Entropy (Normal Mode) Using Amber—Entropy calculations were carried out using Amber 12.0 (MMPBSA.py) (40). All dcd trajectories (NAMD trajectory files) were first converted back into mdcrd files using Amber 12.0 (*ptraj*). Then each mdcrd file consisting of 1000 frames (1 ps/frame) were loaded into MMPBSA.py version 12.0. Key parameters included: nmstartframe = 1; nmendframe = 1000; nminterval = 10; nmode_igb = 1; nmode_istrng = 0.1; drms = 0.0001; maxcyc = 100000; and NMODE frames = 100. Calculations were performed on 10 processors. Total entropy ($T\Delta S$)

TABLE 1
Energy scoring for THC and CBD binding to FABP3, FABP5, and FABP7

Trajectory	ΔE_{VDW} (A)	ΔE_{coul} (B)	ΔG_{polar} (C)	$\Delta G_{nonpolar}$ (D)	MMGBSA (A+B+C+D)	$T\Delta S$ (E)	ΔG_{bind} (A+B+C+D-E)
THC FABP3	−42.81 ± 2.59	−7.29 ± 1.03	18.84 ± 0.67	−4.03 ± 0.03	−35.29 ± 3.54	−19.78 ± 0.83	−15.50 ± 3.22
CBD FABP3	−49.20 ± 1.45	−14.56 ± 1.51	21.15 ± 0.88	−3.88 ± 0.05	−46.48 ± 2.33	−22.85 ± 0.55	−23.64 ± 2.31
THC FABP5	−44.54 ± 1.33	−7.29 ± 1.29	19.27 ± 0.67	−4.07 ± 0.07	−36.63 ± 1.85	−21.35 ± 1.37	−15.28 ± 0.52
CBD FABP5	−45.60 ± 1.06	−13.75 ± 2.91	21.66 ± 1.44	−3.98 ± 0.03	−41.67 ± 0.81	−20.43 ± 0.65	−21.02 ± 0.27
THC FABP7	−45.08 ± 1.26	−8.18 ± 3.14	21.01 ± 1.23	−4.09 ± 0.02	−36.34 ± 3.12	−20.81 ± 0.75	−15.54 ± 3.06
CBD FABP7	−48.43 ± 0.53	−15.78 ± 1.42	24.15 ± 1.23	−3.91 ± 0.04	−43.98 ± 1.23	−21.03 ± 1.10	−22.94 ± 2.25

of the system was calculated from a difference in total energy (translation energy, rotational Energy, and vibrational energy) of the system as shown in Equation 4. Entropy calculations were carried out at 310 K.

$$T\Delta S(310\text{K}) = S_{\text{complex}} - (S_{\text{receptor}} + S_{\text{ligand}}) \quad \text{(Eq. 4)}$$

Enzyme Assays

FAAH activity in homogenates was determined as described previously (11).

AEA Uptake

Inhibition of AEA uptake into cells was performed as described (11). HeLa cells were preincubated with 20 μM THC, CBD, or vehicle (0.1% ethanol in DMEM supplemented with 0.15% BSA) for 15 min followed by incubation with 100 nM [^{14}C]AEA for 5 min. AEA uptake was quantified as previously described (11).

Immunohistochemistry

Brain sections were blocked in 1% serum or 1% nonfat dry milk in PBS-T (0.3% Trition X-100 in PBS) and then incubated with anti-human/mouse serum albumin primary antibody (MAB1455 from R&D Systems used at 1:20) and anti-macrophage/microglia Iba1 (rabbit polyclonal 019-19741 from WakoUSA used at 1:1000) overnight at 4 °C. Incubation with Alexa Fluor 488 and Alexa Fluor 555-conjugated secondary antibodies at 1:1000 was performed at room temperature for 1 h, followed by washing with PBS and mounting using Fluoromount-G with DAPI (Southern Biotech). 4–8 brain sections were imaged per biological replicate.

Statistics

Results represent mean ± S.E. of at least three independent experiments performed in triplicate. Statistical significance was determined using two-tailed unpaired *t* tests against controls or by one-way analysis of variance with post-hoc Dunnett's test compared with vehicle controls (significance set at $p < 0.05$) on the raw data, as indicated. Analysis was performed using GraphPad (version 6.0, Prism).

RESULTS

Computational methods were initially employed to determine the likelihood of FABPs being carriers for cannabinoids. THC and CBD displayed energy scores consistent with appreciable binding to FABP3, FABP5, and FABP7, the main FABPs that are expressed in the brain. This analysis showed tighter binding of CBD to FABP3, FABP5, and FABP7 ($\Delta G_{\text{binding}} = -23.64 \pm 2.31$, -21.02 ± 0.27, and -22.94 ± 2.25 kcal/mol) than did THC ($\Delta G_{\text{binding}} = -15.50 \pm 3.22$, -15.28 ± 0.52, and -15.54 ± 3.06 kcal/mol) (Table 1). THC and CBD were accommodated in the pockets of the FABPs (Fig. 1). Conspicuously, THC binds deeper into the pocket of FABP7 than FABP3 and FABP5. Noticeably, the binding pose is unique for CBD in FABP5 (Fig. 1).

In vitro binding studies of THC and CBD, using a fluorescent NBD-stearate displacement assay, indicated that these two cannabinoids bind to FABP3, FABP5, and FABP7 with low micromolar affinities (Table 2). In addition, for FABP5 there was agreement with the *in silico* results showing that CBD bound more tightly than did THC, however, a significant difference in binding affinities was not observed for FABP3 and FABP7. Interestingly, THC and CBD bind the FABPs as well or nearly as well as the endocannabinoids and a variety of other compounds including various transport inhibitors as discussed below. However, they do not bind as well as many of the fatty acids including oleic acid that binds with nearly 50-fold higher affinity for some of the FABPs (see Table 2).

Because albumin is a known carrier of the cannabinoids in the blood and was proposed to function as an intracellular endocannabinoid-binding protein (9, 15), we examined whether it could function in a similar capacity as an intracellular transporter in the brain by initially examining its expression pattern in the mouse brain. One group has previously reported that microglial cells synthesize albumin (41). Contrary to this report, we did not find any albumin expression in microglia (Fig. 2). In the normal mouse brain albumin expression did not co-localize with the macrophage/microglial marker Iba1, but was rather detected in perivascular areas (Fig. 2, *arrows*). Very low levels of expression could be detected in the cytoplasm of neurons in the hippocampus after extensive incubation with the primary antibody (not shown). These results indicate that albumin is likely not a major intracellular transporter of the cannabinoids in the brain.

We next determined whether FABPs serve as intracellular carriers for THC and CBD. HeLa cells are a suitable cell type to examine interactions of exogenous cannabinoids with FABPs and their effects upon endocannabinoid transport because these cells conveniently express a single FABP subtype, FABP5 (12, 14), AEA uptake is coupled to its breakdown by FAAH (42, 43). Therefore, HeLa cells, which lack FAAH (44), were transfected with human FAAH and AEA uptake was subsequently examined.

Both THC and CBD inhibited AEA uptake, with CBD being slightly more efficacious (Fig. 3*A*). The greater potency of CBD as an inhibitor of AEA uptake mirrored its higher affinity (lower K_i) for FABP5 (Table 2). As expected, FABP5 knockdown inhibited AEA uptake (Fig. 3*A*) (14). Importantly, THC and CBD did not reduce AEA uptake in cells bearing a knockdown of FABP5

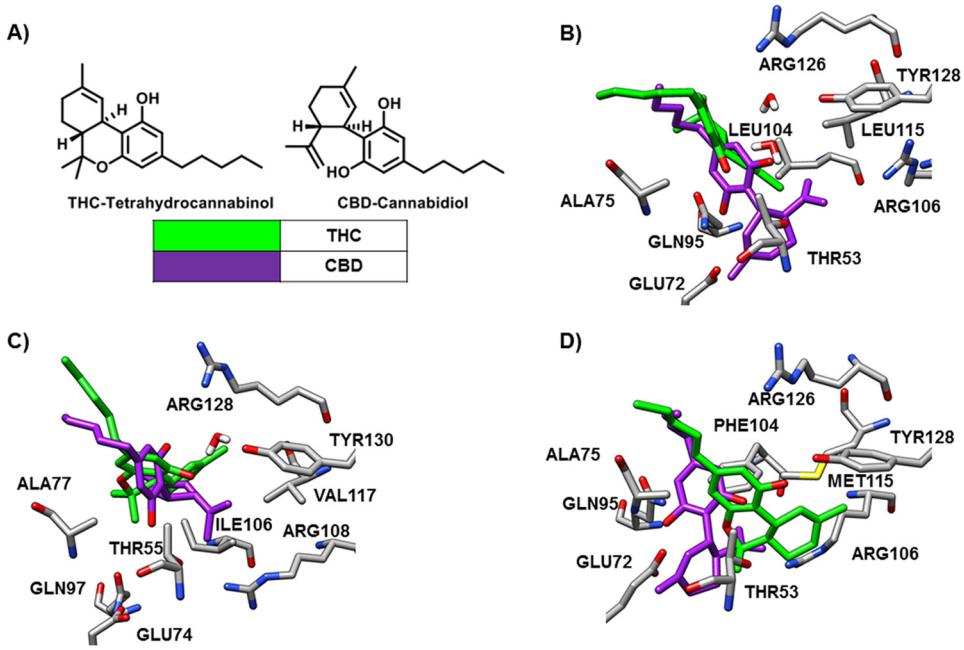

FIGURE 1. **Structures of THC and CBD and the superimposed predicted binding pose for each ligand in FABP3, FABP5, and FABP7.** *A,* chemical structures of THC and CBD. *B,* THC appears sterically crowded in the binding pocket of FABP3 with water-mediated hydrogen bonding seen with TYR128, a key amino acid in the binding of fatty acids. THC instead adopts a direct hydrogen bond with Ala^{75} (2.6 Å). CBD remains in hydrogen bonding distance to Tyr^{128} (5.0 Å), whereas making closer hydrogen bonds through its 1′-OH with Thr^{53} (2.4 Å), Gln^{95} (2.2 Å), and Glu^{72} (3.9 Å). Water-mediated hydrogen bonding with Tyr^{128}, similar to THC, is critical for binding. *C,* THC shows a long-range water mediated hydrogen bonding with Tyr^{130} (5.3 Å), a key amino acid residue critical to FA binding. The Ile^{106} and Val^{117} residues in FABP5 provide less steric hindrance compared with Leu^{104} and Leu^{115} of FABP3, allowing THC to penetrate further into the binding pocket. CBD adopts a unique orientation in FABP5, compared with similar binding poses in FABP3 and FABP7, blocking Tyr^{129} by making a strong hydrogen bond with Arg^{128} (2.1 Å). The 1′-OH of CBD forms hydrogen bonding with Thr^{55}. *D,* THC forms a strong hydrogen bonding directly with Tyr^{128} (2.6 Å), a key amino acid residue critical to fatty acid binding, whereas providing a weaker interaction with Arg^{126} (4.1 Å). The Phe^{104} and Met^{115} residues in FABP7 provide even less steric hindrance compared with similar residues in FABP3 and FABP5, allowing THC to penetrate even further into the binding pocket, which is now without water. CBD adopts a similar binding mode as in FABP3, providing long range interactions between Thr^{53} (2.8 Å) and Tyr^{128} (5.3 Å), whereas additionally providing hydrogen bonding with Ala^{75} (2.3 Å) and Glu^{72} (2.1 Å) via the 1′-OH.

TABLE 2

Binding affinities of THC, CBD, AEA, 2-arachidonoylglycerol (2-AG), and oleic acid (OA) to human FABPs

The K_i values were determined by NBD-stearate fluorescence displacement assays as described under "Experimental Procedures." Values are averages ± S.E. of at least three independent experiments.

Compound	K_i		
	FABP3	FABP5	FABP7
		μM	
CBD	1.69 ± 0.20	1.88 ± 0.10	1.52 ± 0.39
THC	1.98 ± 0.36	3.14 ± 0.26	1.04 ± 0.13
AEA	3.07 ± 0.28	1.26 ± 0.18	0.80 ± 0.06
2-AG	1.65 ± 0.22	1.45 ± 0.21	0.20 ± 0.03
OA	0.04 ± 0.00	0.56 ± 0.14	0.04 ± 0.00

(Fig. 3*A*). Furthermore, THC and CBD did not reduce the proportion of intracellular AEA that is hydrolyzed following uptake, suggesting that the cannabinoids block the delivery of AEA to FAAH but do not affect AEA hydrolysis by FAAH (Fig. 3*B*). In support of this, we found that CBD and THC did not inhibit AEA hydrolysis by human FAAH in cell homogenates (Fig. 3*C*). This result was surprising in light of previous studies demonstrating robust inhibition of rodent FAAH by CBD (17, 45–47). Therefore, we examined whether CBD inhibits rat and mouse FAAH. In agreement with previous studies, CBD inhibited both rat and mouse but not human FAAH (Fig. 3*D*), suggesting a species specificity that may underlie these effects (14, 44).

To further investigate this species specificity, we employed site-directed mutagenesis to interconvert key residues within the active site of human FAAH to the homologous residues found in rat FAAH. Previous work has identified six residues that differ between the active sites of human and rat FAAH (F192L, Y194F, T377A, N435S, V491I, and M495V) (Fig. 4) (48). Of these, Phe^{192} and Met^{495} were identified as likely candidates to alter interactions with CBD based on the crystal structures of human and rat FAAHs with other bound ligands (23). These two residues appeared to restrict the entry of CBD into the active site of human FAAH. Therefore, we mutated these residues in human FAAH to generate F192L, M495V, as well as FAAH bearing the double mutant. Interestingly, the F192L and M495V mutants did not significantly alter FAAH inhibition by CBD. In contrast, human FAAH carrying mutations at both sites was robustly inhibited by CBD, with a similar inhibitor sensitivity profile as seen in rat FAAH (Fig. 5, *A* and *B*).

Computational methods were subsequently employed to characterize the interactions of CBD within the active site of FAAH. CBD was individually docked to human FAAH, rat FAAH, or the F192L/M495V mutant human FAAH, and predicted free energy scores were obtained ($\Delta G_{binding}$ = −26.55 kcal/mol, −36.84 kcal/mol, and −30.46 kcal/mol, respectively). Consistent with the observed biochemical data, CBD was predicted to bind human FAAH with a lower affinity than either rat FAAH or the human FAAH F192L/M495V mutant.

The membrane access channel of FAAH is a cavity of hydrophobic and aromatic residues that connect the catalytic core of the protein to the membrane-associated region, thought to allow lipid substrates to directly access the site of catalysis from

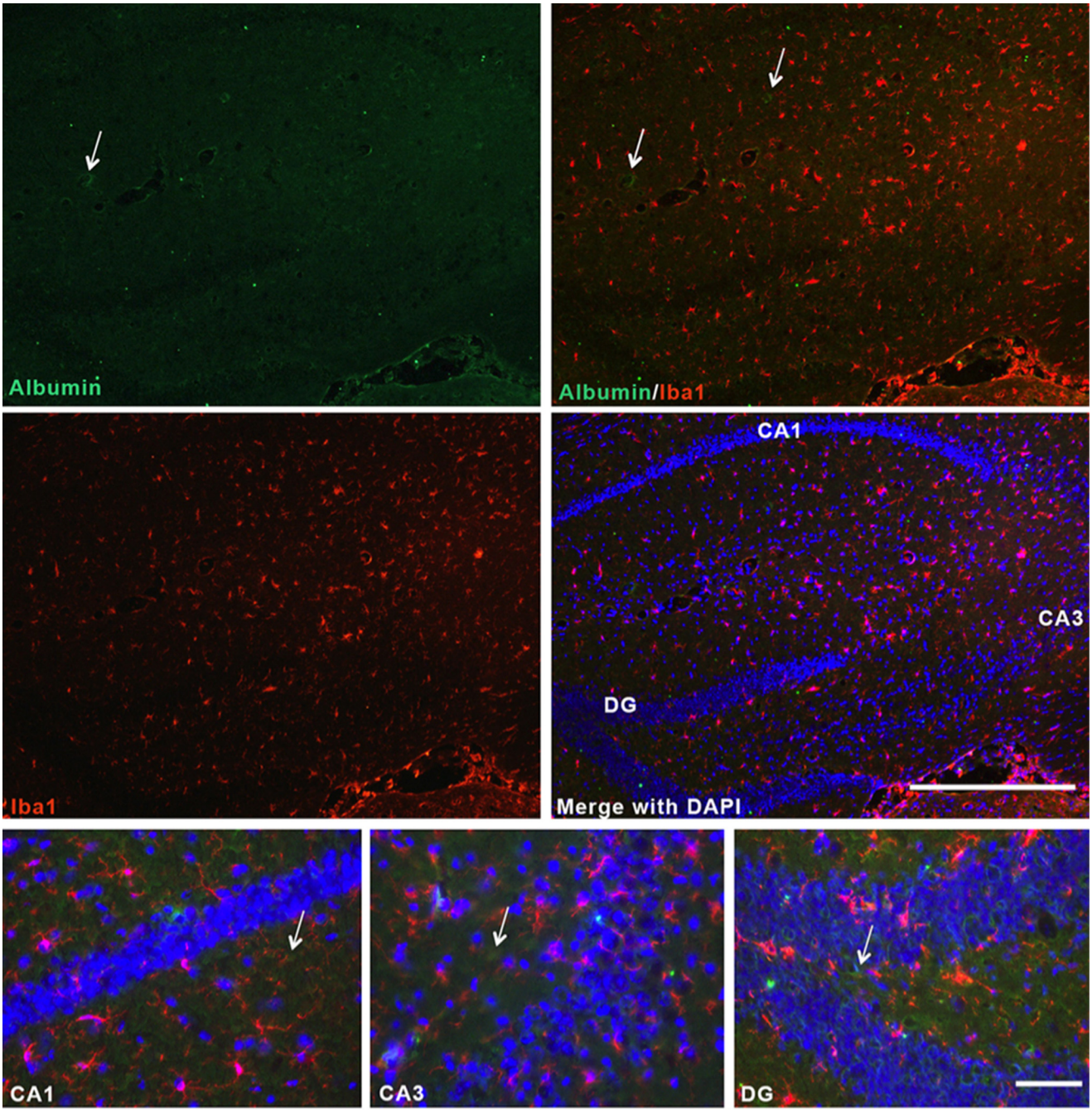

FIGURE 2. **Albumin is not expressed by microglia in the normal mouse brain.** Hippocampal brain sections were obtained from C57Bl6 mice and incubated with anti-albumin and anti-Iba1 antibodies. The sections were incubated with the primary antibody overnight at 4 °C. Images were visualized with Alexa Fluor 488- and Alexa Fluor 555-conjugated secondary antibodies. Nuclei were labeled with DAPI. $n = 4$. *Scale bars*, 500 μm (*upper panels*, low magnification images) and 100 μm (*lower panels*, high magnification images). *Arrows* point to perivascular albumin staining.

the lipid bilayer (49). Substrate catalysis by amidase signature enzymes, such as FAAH, is mediated by an unusual Ser-Ser-Lys catalytic triad (Ser^{241}-Ser^{217}-Lys^{142} in FAAH). Crystal structures of FAAH inhibitors in complex with FAAH reveal these compounds residing within the membrane access channel cavity (49, 50). We performed i*n silico* docking of CBD to FAAH to investigate the preferred binding pose of this cannabinoid. Like other FAAH inhibitors, CBD was predicted to reside within the membrane access channel cavity, coming within 2.8 Å of Ser^{241} of the catalytic core (Fig. 6*A*). AEA was subsequently docked to rat FAAH for comparison and the lowest energy pose was found to be in a highly similar location to that of CBD (Fig. 6*B*), further suggesting the possibility of CBD acting as a competitive inhibitor of FAAH.

Inspection of the predicted geometry of CBD within the active site reveals a twisted conformation of the compound (Fig. 7). Although THC and CBD are isomers, the pyran ring of THC confers added rigidity to the molecule. The reduced structural flexibility of THC should not allow for the same twisted conformation as observed with CBD and likely accounts for the inability of THC to inhibit FAAH activity from either species. Superimposed images of CBD in rat (*red*), human (*blue*), or F192L/

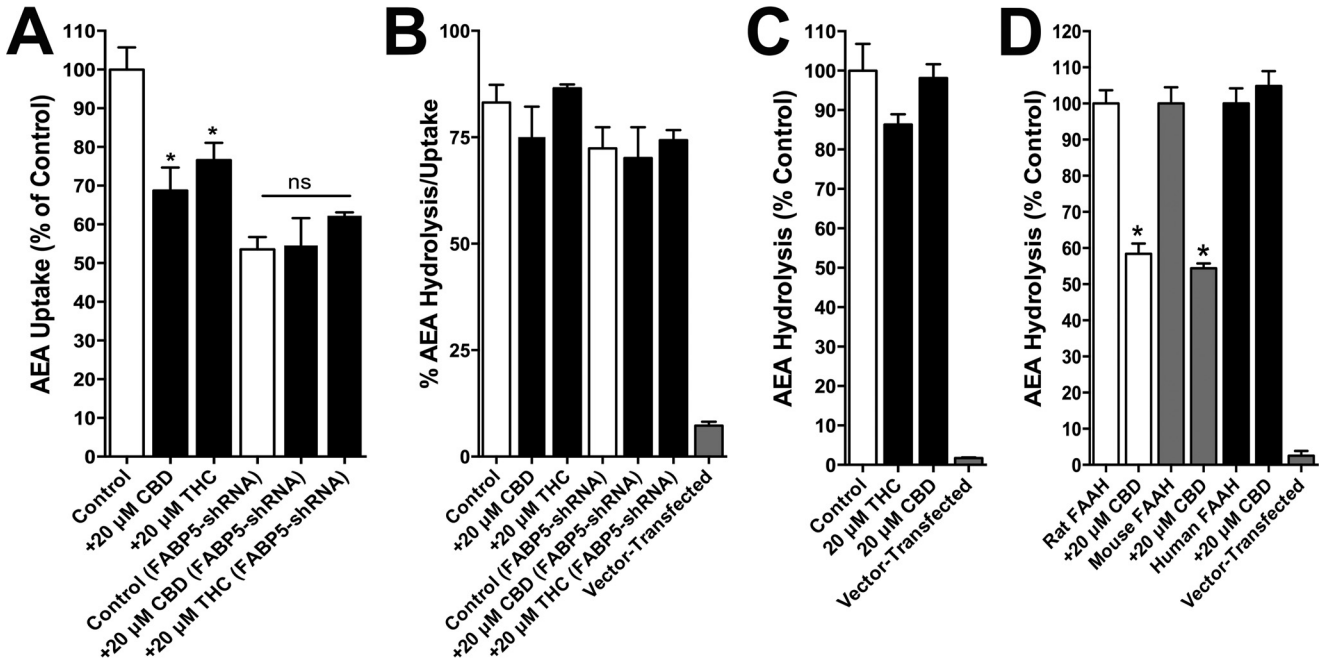

FIGURE 3. **THC and CBD inhibit AEA uptake by targeting FABP5.** *A*, [^{14}C]AEA uptake by human FAAH-transfected WT and FABP5 shRNA-expressing HeLa cells following a 5-min incubation in the presence or absence of 20 μM THC, CBD, or vehicle-only control. *, $p < 0.05$ *versus* control. *B*, ratio of [^{14}C]AEA hydrolysis to total uptake in vector-transfected (*gray*) or human FAAH-transfected WT or FABP5 shRNA HeLa cells following a 5-min incubation in the presence or absence of 20 μM THC, CBD, or vehicle-only control. *C*, [^{14}C]AEA hydrolysis in homogenates of human FAAH-transfected HeLa cells in the absence or presence of 20 μM THC or CBD. *D*, [^{14}C]AEA hydrolysis in homogenates of rat, mouse, or human FAAH-transfected cells in the presence or absence of 20 μM CBD. *, $p < 0.05$.

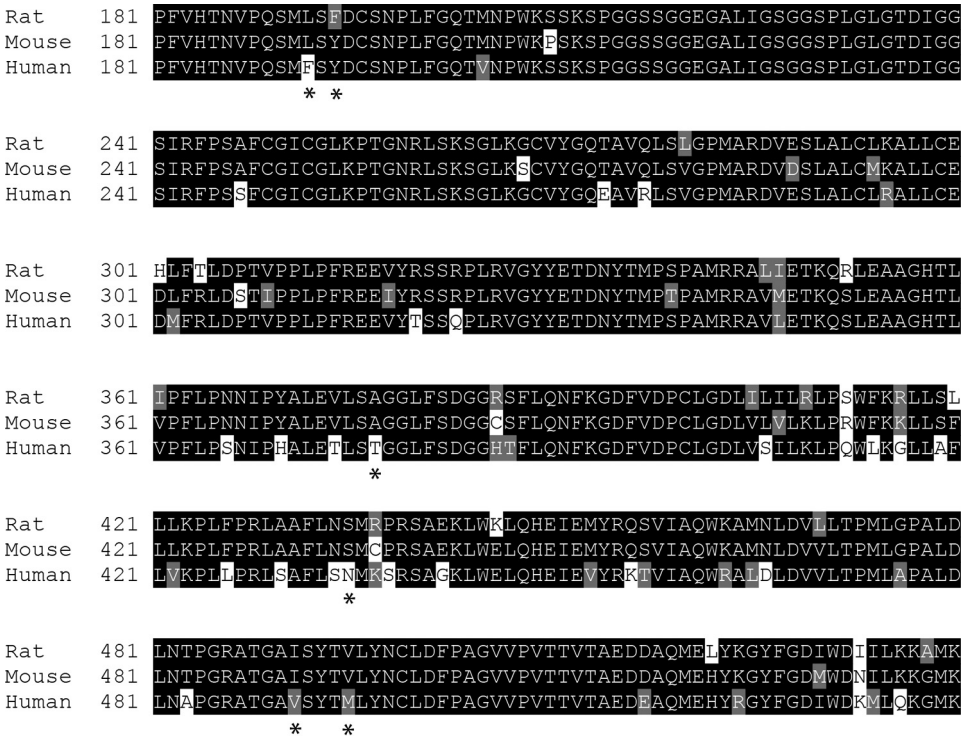

FIGURE 4. **Multiple sequence alignment of human and rodent FAAHs.** Non-homologous residues that reside within the active site are marked with an *asterisk* (*). Sequences were aligned using the ClustalW program and edited with the BOXSHADE (version 3.21) software.

M495V mutant (*purple*) FAAHs reveal similar modes of binding (Fig. 7). CBD penetrates ~1 Å less deeply into the active site of human FAAH and has a less favorable predicted free energy of binding, which may account for it being less potent as an inhibitor in human FAAH in comparison to rat FAAH in our enzyme assays.

DISCUSSION

In the present study, we identified FABPs as the first intracellular carriers for phytocannabinoids and showed that THC and CBD modulate AEA uptake by competing with AEA for binding to FABPs. Therefore, THC and CBD may potentiate AEA signaling by reducing its catabolism. Unexpectedly, in

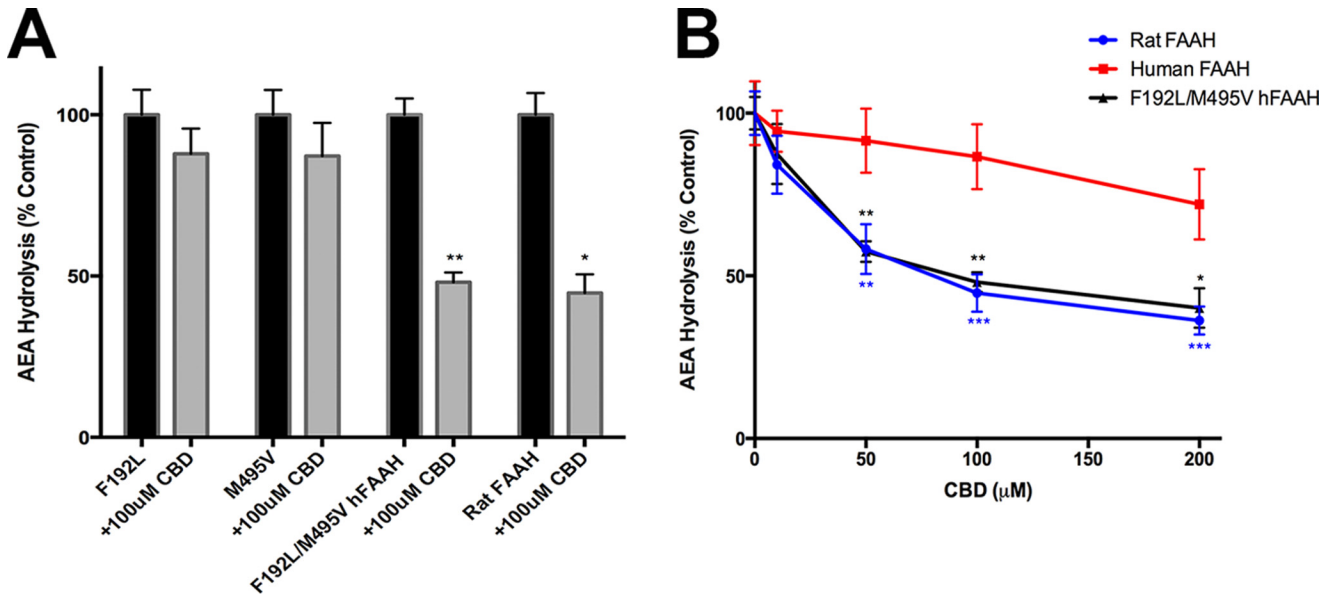

FIGURE 5. **F192L/M495V human FAAH mutant confers sensitivity to inhibition by CBD.** *A*, [^{14}C]AEA hydrolysis in homogenates of rat or mutant FAAH-transfected cells in the presence or absence of 100 μM CBD. *B*, CBD inhibitor sensitivity profile in homogenates of human, rat, or F192L/M495V hFAAH-transfected cells. Data represent the mean ± S.E. for 3 replicates per group. *, $p < 0.05$; **, $p < 0.01$; ***, $p < 0.001$ *versus* vehicle control.

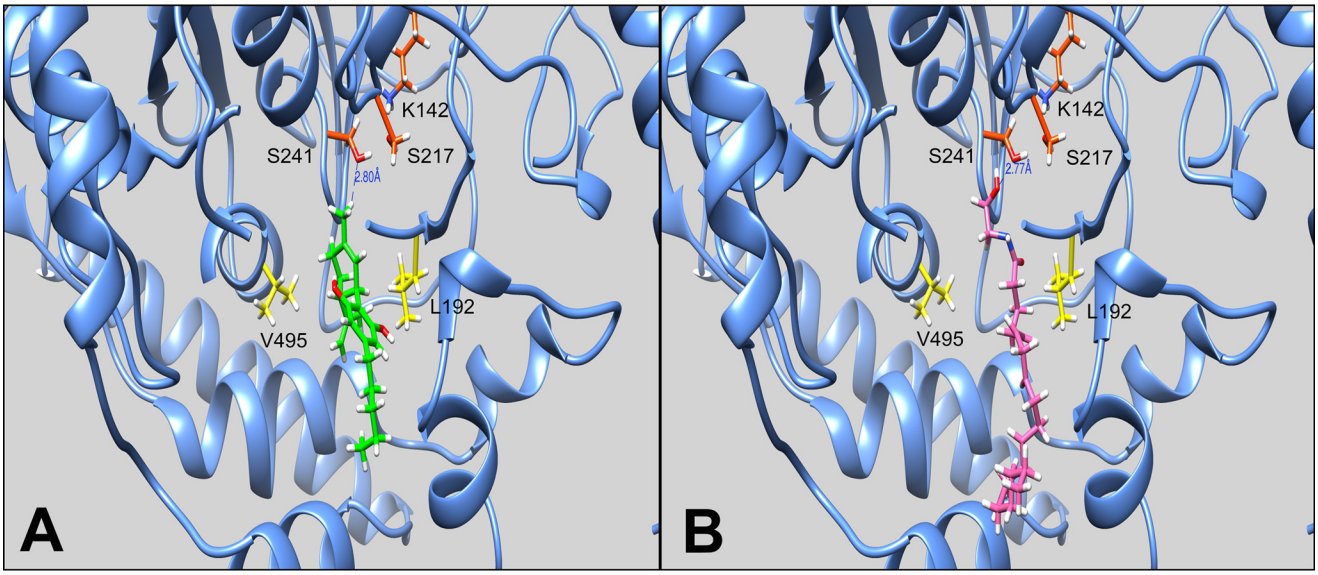

FIGURE 6. **Predicted binding poses of CBD and AEA by *in silico* docking within rat FAAH.** *A*, lowest energy pose of CBD (*green*) within rat FAAH. Depicted residues are the Ser-Ser-Lys catalytic triad (*red*) and two relevant active site residues that differ between rodent and human species (*yellow*). A peripheral section of the protein has been removed for visibility. *B*, lowest energy pose of AEA (*pink*) within rat FAAH. Residues were labeled as in *A*.

contrast to previous reports demonstrating robust inhibition of rodent FAAH by CBD, our findings clearly indicate that FAAH does not serve as a target for CBD in humans. Therefore, the recent observation linking CBD administration to elevated serum AEA levels in humans is unlikely to be attributable to FAAH inhibition, and points to modulation of AEA transport proteins such as FABPs (see schematic in Fig. 8).

In silico modeling demonstrated that THC and CBD interact with FABP3, FABP5, and FABP7 and that both ligands reside within the FABP binding pocket in a manner similar to that shown for AEA and 2-AG by x-ray crystallography (51). *In vitro* experiments confirmed that these cannabinoids bind the FABPs, all with a low micromolar affinity (1.04–3.14 μM). Interestingly, these affinities are only slightly lower than those observed with SBFI26, a truxillic acid compound recently identified as a specific inhibitor of the FABPs (K_i for FABP3, FABP5, and FABP7 = 3.86 ± 0.70, 0.93 ± 0.08, and 0.38 ± 0.04, respectively) (16). However, unlike SBFI26, THC and CBD showed pronounced affinity for FABP3. These two cannabinoids also bind with similar affinities as endocannabinoids AEA and 2-AG (Table 2). The relative similarity in binding affinity between the phytocannabinoids and endocannabinoids suggests that competition for these binding sites may exist. Our results show that the FABPs carry anandamide and that it can be displaced by CBD and THC in milieu of tighter binding of non-esterified fatty acids that, we surmise, are not saturating.

Endocannabinoid signaling is believed to be controlled through a balance of on demand synthesis and prompt catabo-

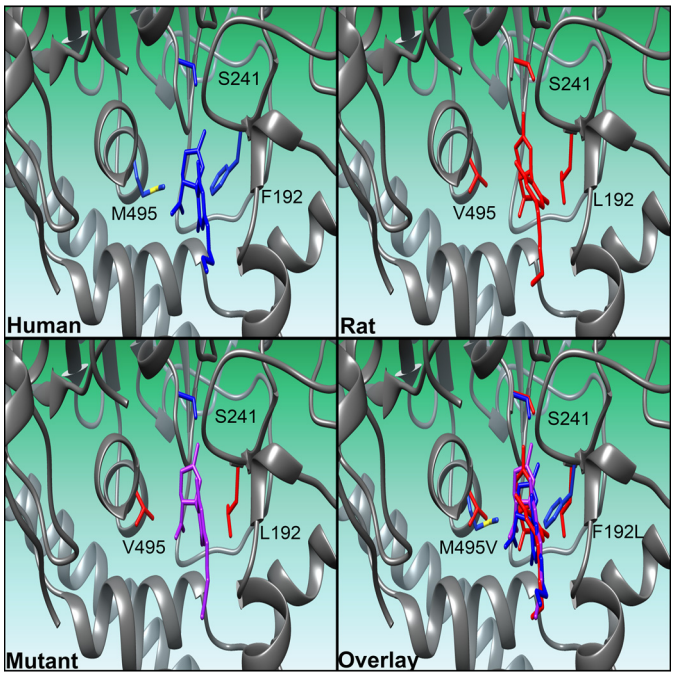

FIGURE 7. **Predicted binding poses of CBD by computational docking within human, rat, or F192L/M495V mutant FAAHs.** Poses of CBD within human, rat, and F192L/M495V human mutant FAAHs reveal similar modes of binding, however, CBD penetrates into the active site of human FAAH slightly less deeply. Compound and residues of human FAAH are shown in *blue*, compound and residues of rat FAAH are shown in *red*, compound docked to the F192L/M495V mutant FAAH are shown in *purple*. A portion of the protein in the depictions has been removed for clarity.

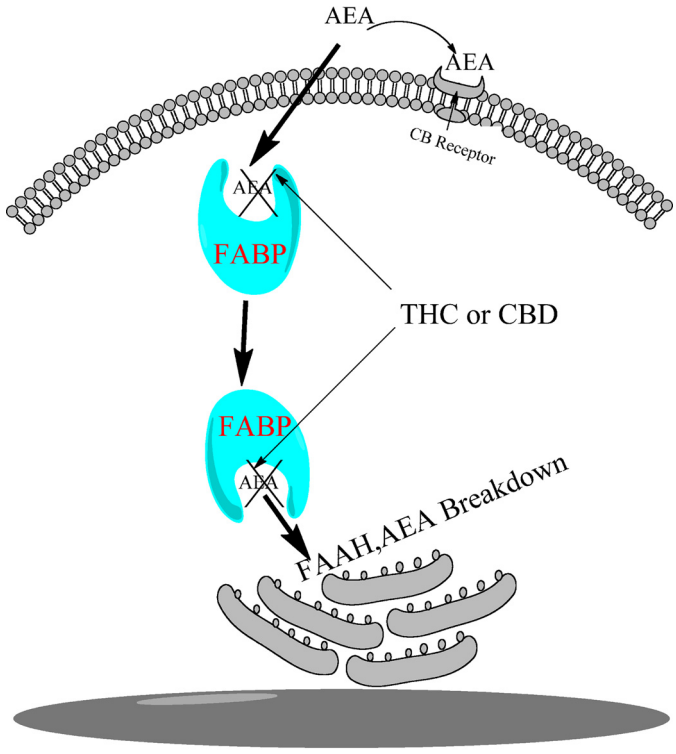

AEA (Anandamide) FAAH (fatty acid amide hydrolase)
FABP (human fatty acid binding protein), CB (cannabinoid receptor)

FIGURE 8. **Conceptual schematic of phytocannabinoids modulating endocannabinoid metabolism via FABP inhibition in human cells.** Endogenous AEA is shuttled through the aqueous environment of the cytoplasm to intracellularly localized FAAH for catabolism. THC and CBD compete for binding to FABPs, thereby reducing the rate of anandamide breakdown and raising AEA levels.

lism (52–55). AEA is inactivated through hydrolysis by intracellular FAAH (56, 57). We chose to employ HeLa cells because they do not express FAAH, and this permitted us to use cells transfected with human, rat, or mouse FAAH. The uptake of AEA is unique compared with other neurotransmitter systems in that AEA does not require a transmembrane transporter. FAAH enzyme activity maintains an inward concentration gradient that drives uptake and this process requires FABPs as carriers (11, 13, 14).

Conveniently, HeLa cells only express a single FABP subtype, FABP5 (12). Our results indicate that CBD and THC inhibit AEA inactivation by targeting FABPs. This is supported by the observations that both phytocannabinoids were without effect in cells bearing a knockdown of FABPs. Furthermore, we did not observe inhibition of human FAAH by either of these cannabinoids.

Previous reports have shown that CBD, but not THC, inhibits mouse and rat FAAH activity (17, 45–47), which we have confirmed here. Unexpectedly, we are the first to report that CBD does not inhibit human FAAH, even at high concentrations. We explored the species-specific differences and found two key residues within the active site of human FAAH that render it resistant to inhibition by CBD.

In addition to exogenous cannabinoids, FABPs bind to endogenous *N*-acylethanolamines related to AEA (12). Therefore, it is not surprising that previous studies have demonstrated that *N*-acylethanolamines that do not themselves activate cannabinoid receptors, potentiate endocannabinoid signaling (58–60). A recent study reported that CBD alleviates the psychotic symptoms of schizophrenia, possibly in part by elevating levels of AEA and *N*-acylethanolamines in humans (17). Another report showed that administration of a single oral dose of 20 mg of THC to 30 healthy volunteers resulted in higher circulating concentrations of anandamide, 2-AG, palmitoyl ethanolamide, and oleoylethanolamide (61). Therefore, it is tempting to speculate that phytocannabinoids modulate the endocannabinoid tone by targeting FABPs in humans (Fig. 8). Indeed, inhibition of FABPs was recently shown to elevate brain levels of AEA in mice (16, 62). This proposed mechanism of AEA modulation in humans is highly dependent on the pharmacological concentrations of cannabinoids in the brain following consumption. To our knowledge there is little data on this front, however, rats administered a low dose (1 mg/kg) of THC or CBD rapidly attained micromolar brain and plasma concentrations of the parent compound and/or their metabolites (63). The reported brain cannabinoid concentrations are above the K_i for the FABPs, indicating the feasibility of a FABP-dependent mechanism of action in modulating endocannabinoid levels.

Following ingestion, THC is biotransformed primarily to the psychoactive metabolite 11-OH-THC, which is further oxidized to the non-psychoactive 11-nor-9-carboxy-THC (THC-COOH). This inactivation pathway primarily occurs by the cytochrome P-450s in the liver, however, extrahepatic metabolism in other tissues such as the brain, intestines, and lungs may

also partially contribute to THC metabolism (64). Phase II metabolism involves glucuronidation of THC-COOH to form soluble adducts that are excreted in urine and feces (10, 64). Phase I metabolism of CBD is similar to that of THC, with primary oxidation at the C-9 position to the alcohol and carboxylic acid, however, little data are available describing its phase II metabolism (64, 65). CBD has been reported to inhibit THC metabolite formation *in vitro* and some groups have found that co-administration of THC and CBD partially inhibits the formation of select THC metabolites in human subjects (66–68).

Metabolic reactions such as phase I hydroxylation by the cytochrome P-450s and phase II glucuronidation occur at the endoplasmic reticulum and, similar to endocannabinoids, phytocannabinoids likely require a carrier for translocation from the cell membrane to the endoplasmic reticulum. In light of our current study, we postulate that FABPs may play a role in trafficking phytocannabinoids through the cytosol to their respective intracellular enzymes, although it is possible that other identified carriers such as HSP70 may also be involved (15).

Cannabinoids have shown promise in treating several neurological disorders, including addiction, anxiety, schizophrenia, and epilepsy, as well as other conditions such as glaucoma, pain, and nausea (4, 5, 17, 69–71). Sativex, an oromucosal spray containing ~1:1 ratio of THC:CBD, has shown promise in treating neuropathic pain and spasticity in patients with multiple sclerosis (26, 72, 73). The efficacy of CBD in the treatment of these various medical conditions suggests that both cannabinoid receptor-dependent and -independent mechanisms of action are at play in conferring such therapeutic benefits. Further studies characterizing the *in vivo* effects of phytocannabinoids are warranted, and the FABPs may emerge as targets of great therapeutic potential in the future of cannabinoid-based pharmacotherapies.

Acknowledgments—We thank Dr. Kyungmin Ji for her immunostaining work and Dr. Robert Rizzo who generously made his facilities available for the computational analysis.

REFERENCES

1. Happyana, N., Agnolet, S., Muntendam, R., Van Dam, A., Schneider, B., and Kayser, O. (2013) Analysis of cannabinoids in laser-microdissected trichomes of medicinal *Cannabis sativa* using LCMS and cryogenic NMR. *Phytochemistry* **87,** 51–59
2. Howlett, A. C., Barth, F., Bonner, T. I., Cabral, G., Casellas, P., Devane, W. A., Felder, C. C., Herkenham, M., Mackie, K., Martin, B. R., Mechoulam, R., and Pertwee, R. G. (2002) International Union of Pharmacology: XXVII. classification of cannabinoid receptors. *Pharmacol. Rev.* **54,** 161–202
3. Pertwee, R. G. (2008) The diverse CB1 and CB2 receptor pharmacology of three plant cannabinoids: Δ9-tetrahydrocannabinol, cannabidiol and Δ9-tetrahydrocannabivarin. *Br. J. Pharmacol.* **153,** 199–215
4. Izzo, A. A., Borrelli, F., Capasso, R., Di Marzo, V., and Mechoulam, R. (2009) Non-psychotropic plant cannabinoids: new therapeutic opportunities from an ancient herb. *Trends Pharmacol. Sci.* **30,** 515–527
5. Mechoulam, R., and Parker, L. A. (2013) The endocannabinoid system and the brain. *Annu. Rev. Psychol.* **64,** 21–47
6. Zanelati, T. V., Biojone, C., Moreira, F. A., Guimarães, F. S., and Joca, S. R. (2010) Antidepressant-like effects of cannabidiol in mice: possible involvement of 5-HT1A receptors. *Br. J. Pharmacol.* **159,** 122–128
7. Hayakawa, K., Mishima, K., Nozako, M., Ogata, A., Hazekawa, M., Liu, A. X., Fujioka, M., Abe, K., Hasebe, N., Egashira, N., Iwasaki, K., and Fujiwara, M. (2007) Repeated treatment with cannabidiol but not Δ9-tetrahydrocannabinol has a neuroprotective effect without the development of tolerance. *Neuropharmacology* **52,** 1079–1087
8. Gomes, F. V., Resstel, L. B., and Guimarães, F. S. (2011) The anxiolytic-like effects of cannabidiol injected into the bed nucleus of the stria terminalis are mediated by 5-HT1A receptors. *Psychopharmacology* **213,** 465–473
9. Fanali, G., Cao, Y., Ascenzi, P., Trezza, V., Rubino, T., Parolaro, D., and Fasano, M. (2011) Binding of Δ9-tetrahydrocannabinol and diazepam to human serum albumin. *IUBMB life* **63,** 446–451
10. Huestis, M. A. (2005) Pharmacokinetics and metabolism of the plant cannabinoids, Δ9-tetrahydrocannabinol, cannabidiol and cannabinol. *Handb. Exp. Pharmacol.* **168,** 657–690
11. Kaczocha, M., Glaser, S. T., and Deutsch, D. G. (2009) Identification of intracellular carriers for the endocannabinoid anandamide. *Proc. Natl. Acad. Sci. U.S.A.* **106,** 6375–6380
12. Kaczocha, M., Vivieca, S., Sun, J., Glaser, S. T., and Deutsch, D. G. (2012) Fatty acid-binding proteins transport *N*-acylethanolamines to nuclear receptors and are targets of endocannabinoid transport inhibitors. *J. Biol. Chem.* **287,** 3415–3424
13. Björklund, E., Blomqvist, A., Hedlin, J., Persson, E., and Fowler, C. J. (2014) Involvement of fatty acid amide hydrolase and fatty acid binding protein 5 in the uptake of anandamide by cell lines with different levels of fatty acid amide hydrolase expression: a pharmacological study. *PloS One* **9,** e103479
14. Berger, W. T., Ralph, B. P., Kaczocha, M., Sun, J., Balius, T. E., Rizzo, R. C., Haj-Dahmane, S., Ojima, I., and Deutsch, D. G. (2012) Targeting fatty acid binding protein (FABP) anandamide transporters: a novel strategy for development of anti-inflammatory and anti-nociceptive drugs. *PLoS One* **7,** e50968
15. Oddi, S., Fezza, F., Pasquariello, N., D'Agostino, A., Catanzaro, G., De Simone, C., Rapino, C., Finazzi-Agrò, A., and Maccarrone, M. (2009) Molecular identification of albumin and Hsp70 as cytosolic anandamide-binding proteins. *Chem. Biol.* **16,** 624–632
16. Kaczocha, M., Rebecchi, M. J., Ralph, B. P., Teng, Y. H., Berger, W. T., Galbavy, W., Elmes, M. W., Glaser, S. T., Wang, L., Rizzo, R. C., Deutsch, D. G., and Ojima, I. (2014) Inhibition of fatty acid binding proteins elevates brain anandamide levels and produces analgesia. *PloS One* **9,** e94200
17. Leweke, F. M., Piomelli, D., Pahlisch, F., Muhl, D., Gerth, C. W., Hoyer, C., Klosterkötter, J., Hellmich, M., and Koethe, D. (2012) Cannabidiol enhances anandamide signaling and alleviates psychotic symptoms of schizophrenia. *Transl. Psychiatry* **2,** e94
18. Furuhashi, M., and Hotamisligil, G. S. (2008) Fatty acid-binding proteins: role in metabolic diseases and potential as drug targets. *Nat. Rev. Drug Discov.* **7,** 489–503
19. Balius, T. E., Mukherjee, S., and Rizzo, R. C. (2011) Implementation and evaluation of a docking-rescoring method using molecular footprint comparisons. *J. Comput. Chem.* **32,** 2273–2289
20. Balendiran, G. K., Schnutgen, F., Scapin, G., Borchers, T., Xhong, N., Lim, K., Godbout, R., Spener, F., and Sacchettini, J. C. (2000) Crystal structure and thermodynamic analysis of human brain fatty acid-binding protein. *J. Biol. Chem.* **275,** 27045–27054
21. Hohoff, C., Börchers, T., Rüstow, B., Spener, F., and van Tilbeurgh, H. (1999) Expression, purification, and crystal structure determination of recombinant human epidermal-type fatty acid binding protein. *Biochemistry* **38,** 12229–12239
22. Min, X., Thibault, S. T., Porter, A. C., Gustin, D. J., Carlson, T. J., Xu, H., Lindstrom, M., Xu, G., Uyeda, C., Ma, Z., Li, Y., Kayser, F., Walker, N. P., and Wang, Z. (2011) Discovery and molecular basis of potent noncovalent inhibitors of fatty acid amide hydrolase (FAAH). *Proc. Natl. Acad. Sci. U.S.A.* **108,** 7379–7384
23. Ahn, K., Johnson, D. S., Mileni, M., Beidler, D., Long, J. Z., McKinney, M. K., Weerapana, E., Sadagopan, N., Liimatta, M., Smith, S. E., Lazerwith, S., Stiff, C., Kamtekar, S., Bhattacharya, K., Zhang, Y., Swaney, S., Van Becelaere, K., Stevens, R. C., and Cravatt, B. F. (2009) Discovery and characterization of a highly selective FAAH inhibitor that reduces inflammatory pain. *Chem. Biol.* **16,** 411–420

24. Pettersen, E. F., Goddard, T. D., Huang, C. C., Couch, G. S., Greenblatt, D. M., Meng, E. C., and Ferrin, T. E. (2004) UCSF Chimera: a visualization system for exploratory research and analysis. *J. Comput. Chem.* **25,** 1605–1612
25. Mukherjee, S., Balius, T. E., and Rizzo, R. C. (2010) Docking validation resources: protein family and ligand flexibility experiments. *J. Chem. Inf. Model.* **50,** 1986–2000
26. Iskedjian, M., Bereza, B., Gordon, A., Piwko, C., and Einarson, T. R. (2007) Meta-analysis of cannabis based treatments for neuropathic and multiple sclerosis-related pain. *Curr. Med. Res. Opin.* **23,** 17–24
27. Huang, Y., and Rizzo, R. C. (2012) A water-based mechanism of specificity and resistance for lapatinib with ErbB family kinases. *Biochemistry* **51,** 2390–2406
28. Phillips, J. C., Braun, R., Wang, W., Gumbart, J., Tajkhorshid, E., Villa, E., Chipot, C., Skeel, R. D., Kalé, L., and Schulten, K. (2005) Scalable molecular dynamics with NAMD. *J. Comput. Chem.* **26,** 1781–1802
29. Case, D. A., Darden, T. A., Cheatham, T. E., Simmerling, C. L., Wang, J., Duke, R. E., Luo, R., Merz, K. M., Wang, B., Pearlman, D. A., Crowley, M., Brozell, S., Tsui, V., Gohlke, H., Mongan, J., Hornak, V., Cui, G., Beroza, P., Schafmeister, C., Caldwell, J. W., Ross, W. S., and Kollman, P. A. (2004) *AMBER8*, University of California, San Francisco
30. Harnak, V., Abel, R., Okur, A., Strockbine, B., Roitberg, A., and Simmerling, C. (2006) Comparison of multiple amber force fields and development of improved protein backbone ParaMETERS. *Proteins* **65,** 712–725
31. Jorgensen, W. L., Chandrasekhar, J., Madura, J. D., Impey, R. W., and Klein, M. L. (1983) Comparison of simple potential functions for simulating liquid water. *J. Chem. Phys.* **79,** 926–935
32. Balius, T. E., and Rizzo, R. C. (2009) Quantitative prediction of fold resistance for inhibitors of EGFR. *Biochemistry* **48,** 8435–8448
33. Feller, S. E., Zhang, Y., Pastor, R. W., and Brooks, B. R. (1995) Constant pressure molecular dynamics simulations: the langevin piston method. *J. Chem. Phys.* **103,** 4613–4621
34. Ryckaert, J.-P., Ciccotti, G., and Berendsen, H. J. C. (1977) Numerical integration of the cartesian equations of motion of a system with constraints: molecular dynamics of *n*-alkanes. *J. Comput. Phys.* **23,** 327–341
35. Darden, T., York, D., and Pedersen, L. (1993) Particle mesh Ewald: an N log(N) method for Ewald sums in large systems. *J. Chem. Phys.* **98,** 10089–10092
36. Srinivasan, J., Cheatham, T. E. I., Cieplak, P., Kollman, P. A., and Case, D. A. (1998) Continuum solvent studies of the stability of DNA, RNA, and phosphoramidate-DNA helices. *J. Am. Chem. Soc.* **120,** 9401–9409
37. Kollman, P. A., Massova, I., Reyes, C., Kuhn, B., Huo, S. H., Chong, L., Lee, M., Lee, T., Duan, Y., Wang, W., Donini, O., Cieplak, P., Srinivasan, J., Case, D. A., and Cheatham, T. E., 3rd (2000) Calculating structures and free energies of complex molecules: combining molecular mechanics and continuum models. *Acc. Chem. Res.* **33,** 889–897
38. Onufriev, A., Bashford, D., and Case, D. A. (2004) Exploring protein native states and large-scale conformational changes with a modified generalized born model. *Proteins* **55,** 383–394
39. Sitkoff, D., Sharp, K. A., and Honig, B. (1994) Accurate calculation of hydration free-energies using macroscopic solvent models. *J. Phys. Chem.* **98,** 1978–1988
40. Case, D. A., Darden, T., Cheatham, T. E. I., Simmerling, C., Wang, J., Duke, R. E., Luo, R., Walker, R. C., Zhang, W., Merz, K. M., Roberts, B. P., Hayik, S., Roitberg, A., Seabra, G., Swails, J., Gotz, A. W., Kolossvary, I., Wong, K. F., Paesani, F., Vanicek, J., Wolf, R. M., Liu, J., Wu, X., Brozell, S. R., Steinbrecher, T., Gohlke, H., Cai, Q., Ye, X., Wang, J., Hsieh, M.-J., Cui, G., Roe, D. R., Mathews, D. H., Seetin, M. G., Salomon-Ferrer, R., Sagui, C., Babin, V., Luchko, T., Gusarov, S., Kovalenko, A., and Kollman, P. A. (2012) *AMBER12*, University of California, San Francisco, CA
41. Ahn, S. M., Byun, K., Cho, K., Kim, J. Y., Yoo, J. S., Kim, D., Paek, S. H., Kim, S. U., Simpson, R. J., and Lee, B. (2008) Human microglial cells synthesize albumin in brain. *PloS One* **3,** e2829
42. Day, T. A., Rakhshan, F., Deutsch, D. G., and Barker, E. L. (2001) Role of fatty acid amide hydrolase in the transport of the endogenous cannabinoid anandamide. *Mol. Pharmacol.* **59,** 1369–1375
43. Deutsch, D. G., Glaser, S. T., Howell, J. M., Kunz, J. S., Puffenbarger, R. A., Hillard, C. J., and Abumrad, N. (2001) The cellular uptake of anandamide is coupled to its breakdown by fatty-acid amide hydrolase. *J. Biol. Chem.* **276,** 6967–6973
44. Kaczocha, M., Glaser, S. T., Chae, J., Brown, D. A., and Deutsch, D. G. (2010) Lipid droplets are novel sites of *N*-acylethanolamine inactivation by fatty acid amide hydrolase-2. *J. Biol. Chem.* **285,** 2796–2806
45. Bisogno, T., Hanus, L., De Petrocellis, L., Tchilibon, S., Ponde, D. E., Brandi, I., Moriello, A. S., Davis, J. B., Mechoulam, R., and Di Marzo, V. (2001) Molecular targets for cannabidiol and its synthetic analogues: effect on vanilloid VR1 receptors and on the cellular uptake and enzymatic hydrolysis of anandamide. *Br. J. Pharmacol.* **134,** 845–852
46. Ligresti, A., Moriello, A. S., Starowicz, K., Matias, I., Pisanti, S., De Petrocellis, L., Laezza, C., Portella, G., Bifulco, M., and Di Marzo, V. (2006) Antitumor activity of plant cannabinoids with emphasis on the effect of cannabidiol on human breast carcinoma. *J. Pharmacol. Exp. Ther.* **318,** 1375–1387
47. De Petrocellis, L., Ligresti, A., Moriello, A. S., Allarà, M., Bisogno, T., Petrosino, S., Stott, C. G., and Di Marzo, V. (2011) Effects of cannabinoids and cannabinoid-enriched *Cannabis* extracts on TRP channels and endocannabinoid metabolic enzymes. *Br. J. Pharmacol.* **163,** 1479–1494
48. Mileni, M., Johnson, D. S., Wang, Z., Everdeen, D. S., Liimatta, M., Pabst, B., Bhattacharya, K., Nugent, R. A., Kamtekar, S., Cravatt, B. F., Ahn, K., and Stevens, R. C. (2008) Structure-guided inhibitor design for human FAAH by interspecies active site conversion. *Proc. Natl. Acad. Sci. U.S.A.* **105,** 12820–12824
49. Bracey, M. H., Hanson, M. A., Masuda, K. R., Stevens, R. C., and Cravatt, B. F. (2002) Structural adaptations in a membrane enzyme that terminates endocannabinoid signaling. *Science* **298,** 1793–1796
50. Mileni, M., Garfunkle, J., DeMartino, J. K., Cravatt, B. F., Boger, D. L., and Stevens, R. C. (2009) Binding and inactivation mechanism of a humanized fatty acid amide hydrolase by α-ketoheterocycle inhibitors revealed from cocrystal structures. *J. Am. Chem. Soc.* **131,** 10497–10506
51. Sanson, B., Wang, T., Sun, J., Wang, L., Kaczocha, M., Ojima, I., Deutsch, D., and Li, H. (2014) Crystallographic study of FABP5 as an intracellular endocannabinoid transporter. *Acta Crystallogr. D Biol. Crystallogr.* **70,** 290–298
52. Di Marzo, V., Melck, D., Bisogno, T., and De Petrocellis, L. (1998) Endocannabinoids: endogenous cannabinoid receptor ligands with neuromodulatory action. *Trends Neurosci.* **21,** 521–528
53. Marsicano, G., Goodenough, S., Monory, K., Hermann, H., Eder, M., Cannich, A., Azad, S. C., Cascio, M. G., Gutiérrez, S. O., van der Stelt, M., López-Rodriguez, M. L., Casanova, E., Schütz, G., Zieglgänsberger, W., Di Marzo, V., Behl, C., and Lutz, B. (2003) CB1 cannabinoid receptors and on-demand defense against excitotoxicity. *Science* **302,** 84–88
54. Basavarajappa, B. S. (2007) Neuropharmacology of the endocannabinoid signaling system: molecular mechanisms, biological actions and synaptic plasticity. *Curr. Neuropharmacol.* **5,** 81–97
55. Howlett, A. C., Reggio, P. H., Childers, S. R., Hampson, R. E., Ulloa, N. M., and Deutsch, D. G. (2011) Endocannabinoid tone *versus* constitutive activity of cannabinoid receptors. *Br. J. Pharmacol.* **163,** 1329–1343
56. Cravatt, B. F., Giang, D. K., Mayfield, S. P., Boger, D. L., Lerner, R. A., and Gilula, N. B. (1996) Molecular characterization of an enzyme that degrades neuromodulatory fatty-acid amides. *Nature* **384,** 83–87
57. Deutsch, D. G., and Chin, S. A. (1993) Enzymatic synthesis and degradation of anandamide, a cannabinoid receptor agonist. *Biochem. Pharmacol.* **46,** 791–796
58. Costa, B., Comelli, F., Bettoni, I., Colleoni, M., and Giagnoni, G. (2008) The endogenous fatty acid amide, palmitoylethanolamide, has anti-allodynic and anti-hyperalgesic effects in a murine model of neuropathic pain: involvement of CB(1), TRPV1 and PPARγ receptors and neurotrophic factors. *Pain* **139,** 541–550
59. García Mdel, C., Adler-Graschinsky, E., and Celuch, S. M. (2009) Enhancement of the hypotensive effects of intrathecally injected endocannabinoids by the entourage compound palmitoylethanolamide. *Eur. J. Pharmacol.* **610,** 75–80
60. Ben-Shabat, S., Fride, E., Sheskin, T., Tamiri, T., Rhee, M. H., Vogel, Z., Bisogno, T., De Petrocellis, L., Di Marzo, V., and Mechoulam, R. (1998) An entourage effect: inactive endogenous fatty acid glycerol esters enhance

2-arachidonoyl-glycerol cannabinoid activity. *Eur. J. Pharmacol.* **353,** 23–31
61. Walter, C., Ferreirós, N., Bishay, P., Geisslinger, G., Tegeder, I., and Lötsch, J. (2013) Exogenous Δ(9)-tetrahydrocannabinol influences circulating endogenous cannabinoids in humans. *J. Clin. Psychopharmacol.* **33,** 699–705
62. Yu, S., Levi, L., Casadesus, G., Kunos, G., and Noy, N. (2014) Fatty acid-binding protein 5 (FABP5) regulates cognitive function both by decreasing anandamide levels and by activating the nuclear receptor peroxisome proliferator-activated receptor β/δ (PPARβ/δ) in the brain. *J. Biol. Chem.* **289,** 12748–12758
63. Alozie, S. O., Martin, B. R., Harris, L. S., and Dewey, W. L. (1980) ^{3}H-Δ9-Tetrahydrocannabinol, ^{3}H-cannabinol and ^{3}H-cannabidiol: penetration and regional distribution in rat brain. *Pharmacol. Biochem. Behav.* **12,** 217–221
64. Huestis, M. A. (2007) Human cannabinoid pharmacokinetics. *Chem. Biodiversity* **4,** 1770–1804
65. Bergamaschi, M. M., Barnes, A., Queiroz, R. H., Hurd, Y. L., and Huestis, M. A. (2013) Impact of enzymatic and alkaline hydrolysis on CBD concentration in urine. *Anal. Bioanal. Chem.* **405,** 4679–4689
66. Hunt, C. A., Jones, R. T., Herning, R. I., and Bachman, J. (1981) Evidence that cannabidiol does not significantly alter the pharmacokinetics of tetrahydrocannabinol in man. *J. Pharmacokinetics Biopharmaceutics* **9,** 245–260
67. Nadulski, T., Pragst, F., Weinberg, G., Roser, P., Schnelle, M., Fronk, E. M., and Stadelmann, A. M. (2005) Randomized, double-blind, placebo-controlled study about the effects of cannabidiol (CBD) on the pharmacokinetics of Δ9-tetrahydrocannabinol (THC) after oral application of THC *versus* standardized cannabis extract. *Therap. Drug Monitoring* **27,** 799–810
68. McArdle, K., Mackie, P., Pertwee, R., Guy, G., Whittle, B., and Hawksworth, G. (2001) Selective inhibition of Δ(9)-tetrahydrocannabinol metabolite formation by cannabidiol *in vitro*. *Toxicology* **168,** 133–134
69. Meiri, E., Jhangiani, H., Vredenburgh, J. J., Barbato, L. M., Carter, F. J., Yang, H. M., and Baranowski, V. (2007) Efficacy of dronabinol alone and in combination with ondansetron *versus* ondansetron alone for delayed chemotherapy-induced nausea and vomiting. *Curr. Med. Res. Opin.* **23,** 533–543
70. Tomida, I., Azuara-Blanco, A., House, H., Flint, M., Pertwee, R. G., and Robson, P. J. (2006) Effect of sublingual application of cannabinoids on intraocular pressure: a pilot study. *J. Glaucoma* **15,** 349–353
71. Devinsky, O., Cilio, M. R., Cross, H., Fernandez-Ruiz, J., French, J., Hill, C., Katz, R., Di Marzo, V., Jutras-Aswad, D., Notcutt, W. G., Martinez-Orgado, J., Robson, P. J., Rohrback, B. G., Thiele, E., Whalley, B., and Friedman, D. (2014) Cannabidiol: pharmacology and potential therapeutic role in epilepsy and other neuropsychiatric disorders. *Epilepsia* **55,** 791–802
72. Langford, R. M., Mares, J., Novotna, A., Vachova, M., Novakova, I., Notcutt, W., and Ratcliffe, S. (2013) A double-blind, randomized, placebo-controlled, parallel-group study of THC/CBD oromucosal spray in combination with the existing treatment regimen, in the relief of central neuropathic pain in patients with multiple sclerosis. *J. Neurol.* **260,** 984–997
73. Collin, C., Davies, P., Mutiboko, I. K., Ratcliffe, S., and Sativex Spasticity in MS Study Group (2007) Randomized controlled trial of cannabis-based medicine in spasticity caused by multiple sclerosis. *Eur. J. Neurol.* **14,** 290–296

Fatty Acid-binding Proteins (FABPs) Are Intracellular Carriers for Δ^9-Tetrahydrocannabinol (THC) and Cannabidiol (CBD)

Matthew W. Elmes, Martin Kaczocha, William T. Berger, KwanNok Leung, Brian P. Ralph, Liqun Wang, Joseph M. Sweeney, Jeremy T. Miyauchi, Stella E. Tsirka, Iwao Ojima and Dale G. Deutsch

J. Biol. Chem. 2015, 290:8711-8721.
doi: 10.1074/jbc.M114.618447 originally published online February 9, 2015
